Electronic Supplementary Information for

Characterization of a NanoGland for the Autotransplantation of Human Pancreatic Islets

Omaima M. Sabek[a,b,#], *Silvia Ferrati* [c,#], *Daniel W. Fraga*[a], *Juliana Sih*[c], *Erika V. Zabre*[c], *Daniel H. Fine*[c], *Mauro Ferrari*[c,d,e,f], *Osama A. Gaber*[a,g], *Alessandro Grattoni* [c,*].

[#] *equal contribution* [*] *corresponding author*

[a]Department of Surgery, The Methodist Hospital, 6565 Fannin Street, Houston, TX 77030, USA.
[b]Department of Cell and Molecular biology Weill Cornell Medical College, 1300 York Avenue. New York, NY 10065, USA.
[c]Department of Nanomedicine, The Methodist Hospital Research Institute, 6670 Bertner Ave., Houston, TX 77030, USA.
[d]Department of Medicine, Weill Cornell Medical College, 1300 York Avenue. New York, NY 10065, USA.
[e]Department of Bioengineering, Rice University, 6100 Main Street Houston, TX 77251, USA.
[f]Alliance for NanoHealth, 6670 Bertner Ave., Houston, TX 77030, USA.
[g]Department of Surgery, Weill Cornell Medical College, 1300 York Avenue. New York, NY 10065, USA.

Section 1- Mathematical Model

Glucose Diffusivity

The diffusivity of glucose is concentration dependent[1]. The data of diffusivity scaling with concentration are shown in Supplementary Table 1.

Supplementary Table 1. *Glucose diffusivity scaling with concentration*

c, μg mL^{-1}	c, M	Gladden
0	0	6.75168E-06
162144	0.9	5.19543E-06
317081.6	1.76	3.77984E-06
666592	3.7	8.43071E-07

However, in our experiments the glucose concentration was kept within the range of 0 to 400 μg mL^{-1} corresponding to small molar concentration in the range from 0 to 2.2*10^{-3}, respectively. At the maximum concentration of 400 μg mL^{-1} the diffusivity of glucose corresponds to 6.748*10^{-6} cm^2 s^{-1}. Thus, in first approximation, we considered the glucose bulk diffusivity of 6.75*10^{-6} cm^2 s^{-1} valid for all concentration within the range 0-400 μg mL^{-1}, used in our study. In order to predict the glucose diffusion kinetics across the nanochannel membranes, we took into account the effect of physical and electrostatic confinement operated by channels on glucose diffusivity in 3.6, 5.7, 13, 20, 40 nm nanochannels and, 20, 40 and 60 μm. The diffusivity values in nanoconfinement were obtained by considering the hindrance-theory of molecules through *slit*-nanochannels presented by Deen[2]. The hindrance factor H was calculated as a

function of λ, defined as the molecule hydrodynamic diameter to channel size ratio. Numerous studies have reported on the hydrodynamic radius of glucose. Supplementary Table 2 lists a few literature values.

Supplementary Table 2. *Literature data of glucose hydrodynamic diameter.*

Source	Hydrodynamic Radius (Å)
Peppenheimer *et al.*[3]	3.8
Bouchoux *et al.*[4]	3.65
Stuart[5]	3.9
Schultz Viscosity[6]	4.2
Stokes Einstein	3.6

A glucose hydrodynamic radius, r_h, of 3.9 Å was ultimately used, which takes into account the Stuart and Briegleb correction [5] to the Stokes-Einstein predicted value, required in the case of comparable molecular volumes between solute and solvent. The calculated hindrance factors and related glucose diffusivity in confinement are listed in Supplementary Table 3.

Supplementary Table 3. *Glucose diffusivity in micro- and nanochannel according to the hindrance theory of Deen and molecular dynamics calculations from Ziemys et al.*

R_h	CH size (nm)	λ	H	Deen, D cm^2 s^{-1} (10^{-6})	Ziemys, D cm^2 s^{-1} (10^{-6})
0.39	3.6	2.17E-01	0.62	4.16	4.13
	5.7	1.37E-01	0.75	5.03	5.40
	13	6.00E-02	0.88	5.96	6.60
	20	3.90E-02	0.92	6.23	6.73
	40	1.95E-02	0.96	6.49	6.75
	20,000	3.90E-05	1.00	6.75	6.75
	40,000	1.95E-05	1.00	6.75	6.75
	60,000	1.30E-05	1.00	6.75	6.75

According to the hindrance factor calculation, the effect of nanoscale on glucose diffusivity is significant exclusively for channels smaller than 40 nm. In larger channel, glucose diffusivity can be considered equal to the bulk value. Similar results were obtained by Ziemys *et al.*[7, 8] by means of molecular dynamics simulations. Ziemys data were here fit with the exponential function

$$D_{eff} = D_{bulk}(1 - e^{-\beta(h-d_h)}) \qquad (1)$$

to extrapolate the effective diffusivities (D_{eff}) at the various nanochannel sizes, h. In (2) D_{bulk} corresponds to the diffusivity of glucose in solution in a 3-dimensional space free of rigid physical boundaries (channel walls), d_h is the hydrodynamic diameter of glucose and β the fitting parameter. The obtained values, listed in Supplementary Table 3, show a similar trend to the hindrance predicted values with a maximum difference of approximately 9.6% in correspondence to the 13 nm nanochannel. Supplementary Figure 1 shows the diffusivity scaling for glucose as predicted by Deen and Ziemys. The finding of Ziemys *et al.* relates to the case of glucose in nanoconfinement and is not directly applicable to other molecules, such as insulin, without specific molecular dynamics simulation. As shown by the comparison with Ziemys work, Deen's hindrance theory, although less specific, produces reasonable estimates and can be applied to a broad spectrum of molecules in confinement. For this reason in this work we adopt Deen's hindrance theory for both the case of glucose and insulin diffusive transport across nanoscale channels. The above considerations are valid for a purely diffusive transport of molecules. In the case of large microchannels (20, 40 and 60 μm) convective transport becomes significant and the diffusivity has to be replaced by an apparent diffusivity D_A, which takes into account convective flows associated to the experimental setup. These can be related to differences in fluid density or fluid mixing. Values of D_A cannot be easily theoretically calculated but must be experimentally determined. For this we performed glucose transport experiments as later detailed in section "*In Vitro* Glucose Release Test". The experimental results provided us with a convective factor $\delta = D_A/D$. D_A and δ data are available in the manuscript.

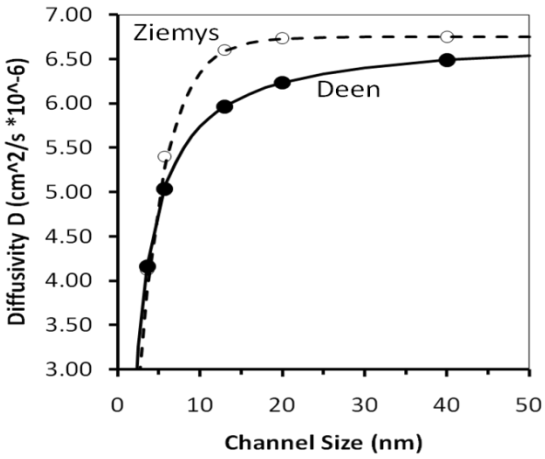

Figure S1. Glucose diffusivity scaling prediction from Deen and Ziemys.

Glucose-Stimulated Insulin Secretion

Stimulated by the increasing glucose concentration islets start releasing insulin within the NanoGland. Insulin then diffuses through the micro- and nanochannels toward the outside environment where its concentration is measured. Literature data report the islet characteristic insulin production profile as a function of the experienced glucose concentration. Specifically, Harrison *et al.* showed a sigmoidal stimulation of insulin release[9] (Supplementary Figure 2). Data experimentally obtained by Harrison *et al.* with human islets, were fit by a sigmoidal curve (correlation coefficient R =0.998):

$$I(c_G) = \frac{\alpha(c-c_0)}{\sqrt{\beta+(c-c_0)^2}} + \gamma \qquad (2)$$

where α, β, γ and c_0 are the fitting coefficients (α=48.75 μU islet^{-1}hour^{1}; β=257,964 μg^2 mL^{-2}; γ = 67.69 μU islet^{-1}hour^{1}; c_0=886.04 μg mL^{-1}).

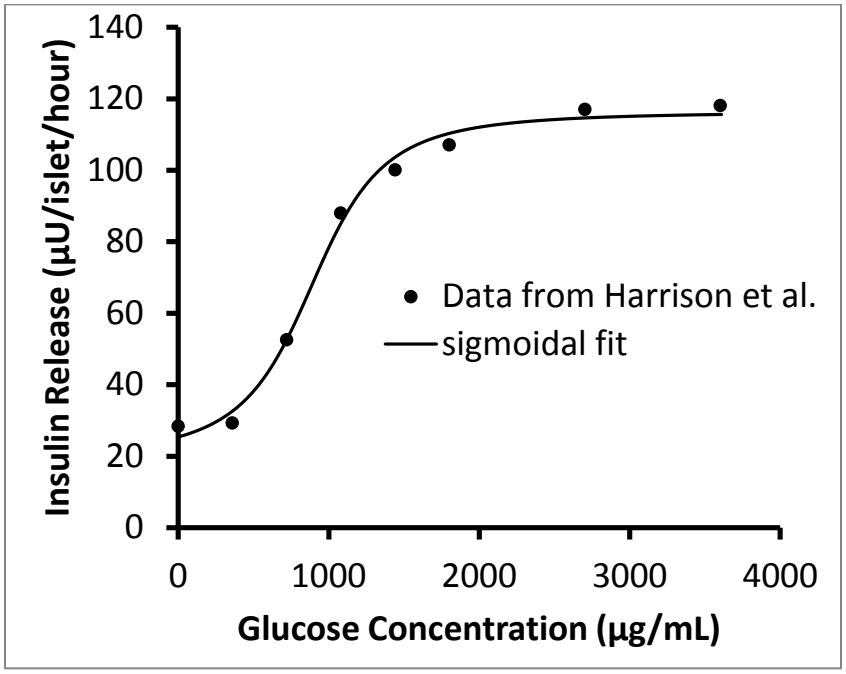

Figure S2. Stimulation data of insulin release from human islet obtained from Harrison *et al.*

Insulin Diffusivity

To model the insulin release from the NanoGland, diffusion properties of insulin through micro- and nanochannels were taken into account. As performed for glucose, Deen's hindrance theory was used to estimate insulin diffusivity scaling in micro- and nanochannels. The quaternary structure of insulin under physiological conditions (pH 6-7) is hexameric[10] with a hydrodynamic radius r_h = 2.86 nm[11].

Supplementary Table 4. *Literature data of hydrodynamic radius r_h and bulk diffusivity D_∞ of insulin.*

Reference	R_h	D_∞
Fabrice Gritti. The mass transfer mechanism of column packed with sub-3 um shell particles and its reproducibility for low and high-molecular weights compounds. Chromathogaphy Today		Hexamer 1.29 x 10^{-6} cm^2 s^{-1}
Polson A.J. (1950) Journal phys Colloid chem 54,649-652		Hexamer 1.3x10^{-6} cm^2 s^{-1}
www.wyat.com/files/literature/Dyanmic_Light _Scattering-202-insulin.pdf	2.59 nm hexamer	
www.malvern.co.uk	2.69 nm hexamer	
Bohidar. Light scattering study of solution properties of bovine serum albumin, insulin and polystyrene under moderate pressure. Colloid & Polymer Science	2.9 nm pH 7.4	0.7x10^{-6} cm^2 s^{-1}
Hosoya *et al.*, Determination of diffusion coefficients of peptides and prediction of permeability through a porous membrane. J. Pharmacy and Pharmacology. (2004)	2.862 nm	1.14 x10^{-6} cm^2 s^{-1} pH 7.4
Seki *et al.* (2003)Measurement of diffusion coefficients of parabens and steroids in water and l-octanol. *Chem Pharma Bull.*		Hexamer 0.933 x10^{-6} cm^2 s^{-1}

Good agreement was found among literature data of hydrodynamic radius r_h and bulk diffusivity D_∞ of insulin (see Supplementary Table 4). Supplementary Table 5 lists and Supplementary Figure 3 graphs the scaled diffusivity values for insulin hexamer at physiologic conditions as calculated through Deen's hindrance theory, by considering a bulk diffusion coefficient D_∞=1.14*10^{-6} cm^2 s^{-1}.

Supplementary Table 5. *Scaled diffusivity values for insulin hexamer at physiologic conditions as calculated through Deen's hindrance theory.*

R	nCH size	Lamda	H	D cm^2 s^{-1} (10^{-6})
2.86	5.7	1.00	0.00	0.00
	13	0.44	0.34	0.38
	20	0.29	0.52	0.59
	40	0.14	0.74	0.84
	1000	0.01	0.99	1.13
	20000	0.00	1.00	1.14
	40000	0.00	1.00	1.14
	60000	0.00	1.00	1.14

As shown by the tabulated values, the confinement of insulin is negligible at the microscale and starts been significant below 100 nm nanochannels.

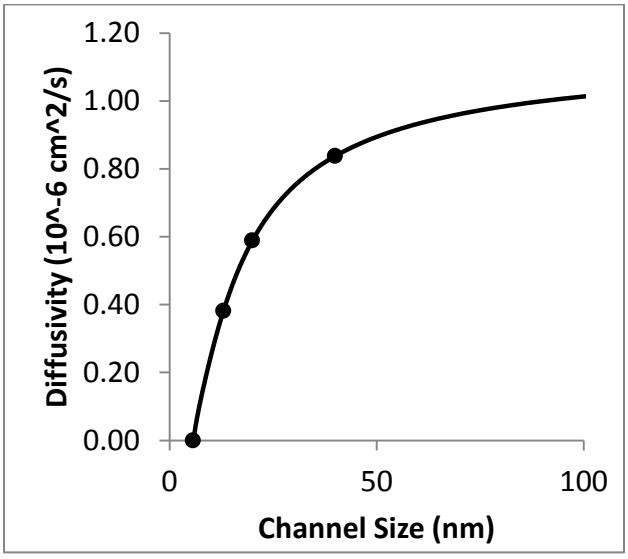

Figure S3. Insulin scaled diffusivity.

While for nanochannels the scaled diffusivities determined by Deen's hindrance theory were adopted, for microchannels apparent diffusivity values $D_A=\delta D$ were employed. Insulin release characteristics from micro- and nanochannel membranes were calculated as previously done for glucose. The proportionality parameter, ε, between insulin concentration gradient and release rate was computed and its values are listed in Supplementary Table 6 for each channel size.

Supplementary Table 6. *Proportionality parameter, ε, between insulin concentration gradient and release rate.*

Channel Size	**ε (μg hour^{-1})/(μg mL^{-1})**
3.6	0.0E+00
5.7	0.0E+00
13	0.0041
20	0.0080
40	0.0143
20 μm	0.0721
40 μm	0.1840
60 μm	0.3812

Section 2- *In vitro* Experiments

In Vitro Glucose Release Test

Glucose diffusion through our 60, 40 and 20 µm, and 40 nm channel size membranes was tested *in vitro*. Membranes were epoxied within a cylindrical titanium capsules, as previously described[12]. Capsules were sealed, loaded with a glucose solution (40 mg mL^{-1}) and immersed into a bicker containing with 14 mL of 0.2 mg mL^{-1} glucose solution. The outside solution was continuously stirred by means of a magnetic stirring bar and frequently sampled (5 µL) and analyzed for glucose content with a commercially available glucose meter (Abbott FreeStyle Lite Blood Glucose Meter).

Human Pancreatic Islets

Islets were obtained from donors and isolated as previously described in the literature[13-20].

NanoGland Assembly

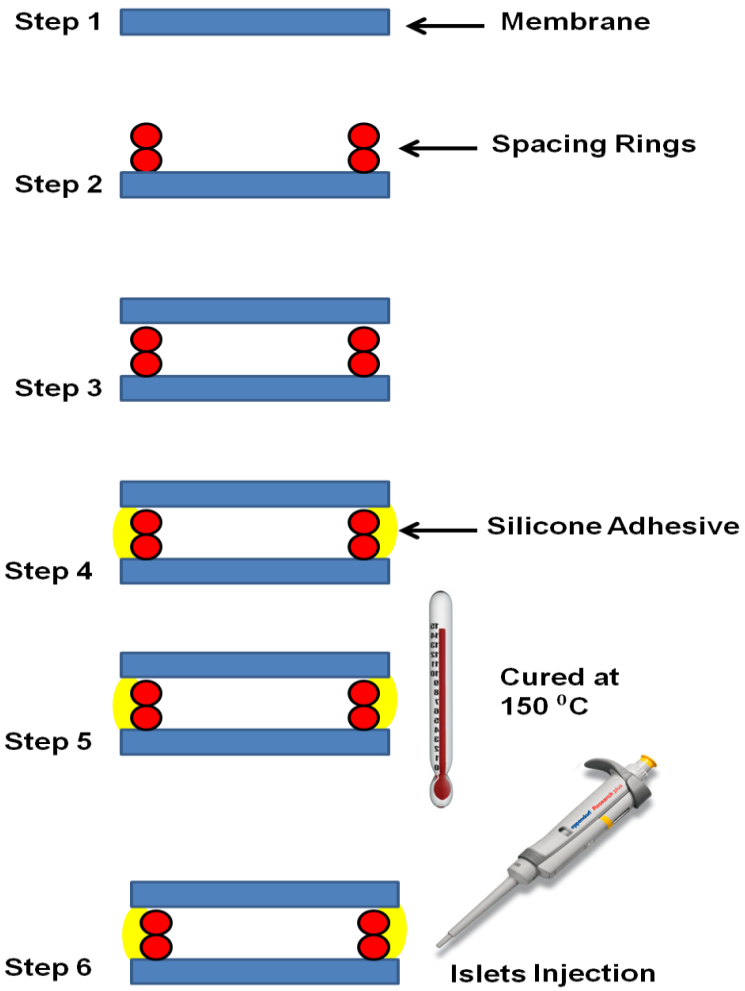

Figure S4. Flow process of NanoGland Assembly starting from two identical silicon nanochannel membranes.

Human Islets Viability *in Vitro*

Perfusion Apparatus

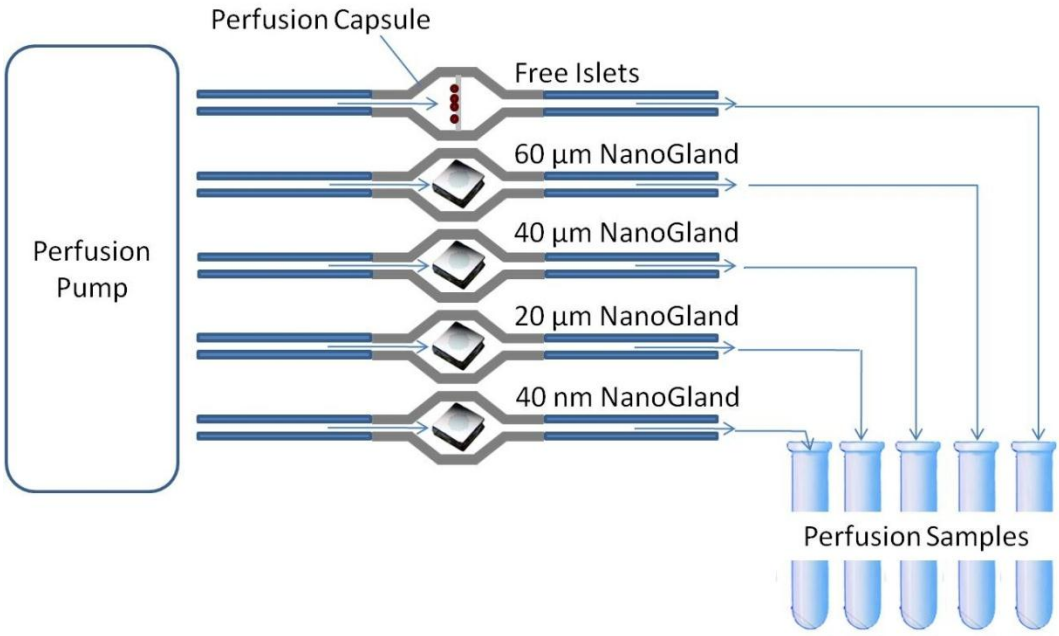

Figure S5. Apparatus to assess insulin secretion in response to glucose challenge, under perfusion conditions. 50-100 IEQ either free or loaded into NanoGlands (3, 5, 13, 20, 40 nm, 20, 40, and 60 µm) were inserted into the chamber at day 21. The Islets were subjected to the following media cycle: initial low-glucose media (30 mg dL^{-1}), constant flow (1.0 mL min^{-1}) of low-glucose solution at 37°C for one hour, high-glucose solution (400 mg dL^{-1}) for two hours, low-glucose for additional 60 minutes. During the procedure, samples of the effluent medium were collected every 10 minutes and analyzed for insulin released.

NanoGland Islets Retention

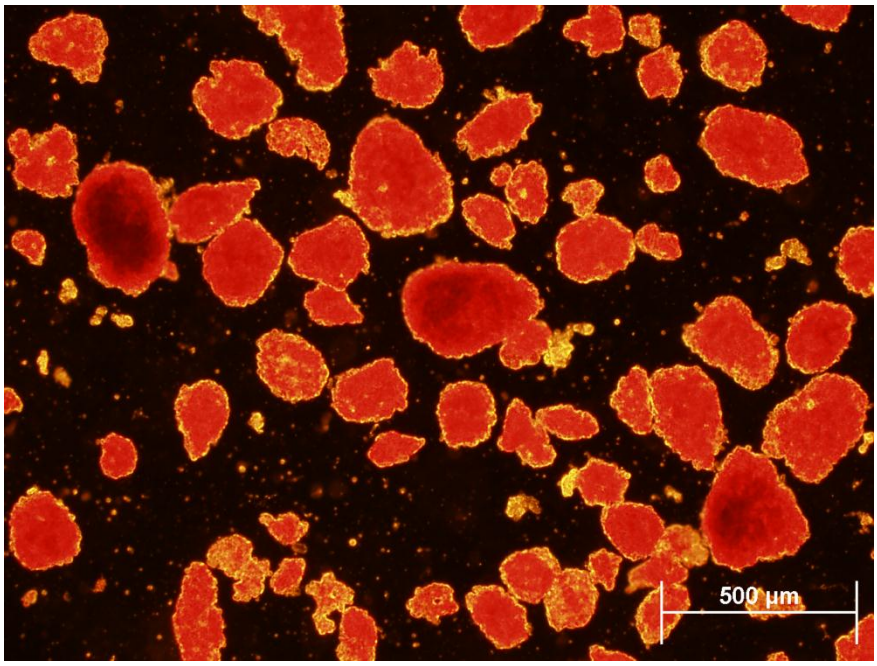

Figure S6. Representative image of zinc-stained human islets used to assess size distribution by means of imaging software (Adobe Photoshop and ImageJ)

Section 3- *In vivo* Experiments

Viability of NanoGland-transplanted Islets

Insulin Measurement Elisa Kit

Thirty minutes after glucose injection, animals blood samples were collected to quantify human specific insulin in plasma using ELISA assay (Alpco Diagnostics, Salem, NH). The Human insulin ELISA presented negligible cross-reactivity to mouse insulin (< 1.0%) as demonstrated by extensive validation in over 2,000 NOD-scid and NUDE mice prior this study[14, 16]. Assay background level of human insulin, measured in mice pre-transplant, was 1.62 ± 1.21µU mL^{-1}. For evaluation of islets *in vivo* viability, human insulin values bigger than 5.0 uU mL^{-1} in tested mice (mean + 2 standard deviations above the background level) were consistent with functional islet grafts.

Human Insulin levels *in vivo*

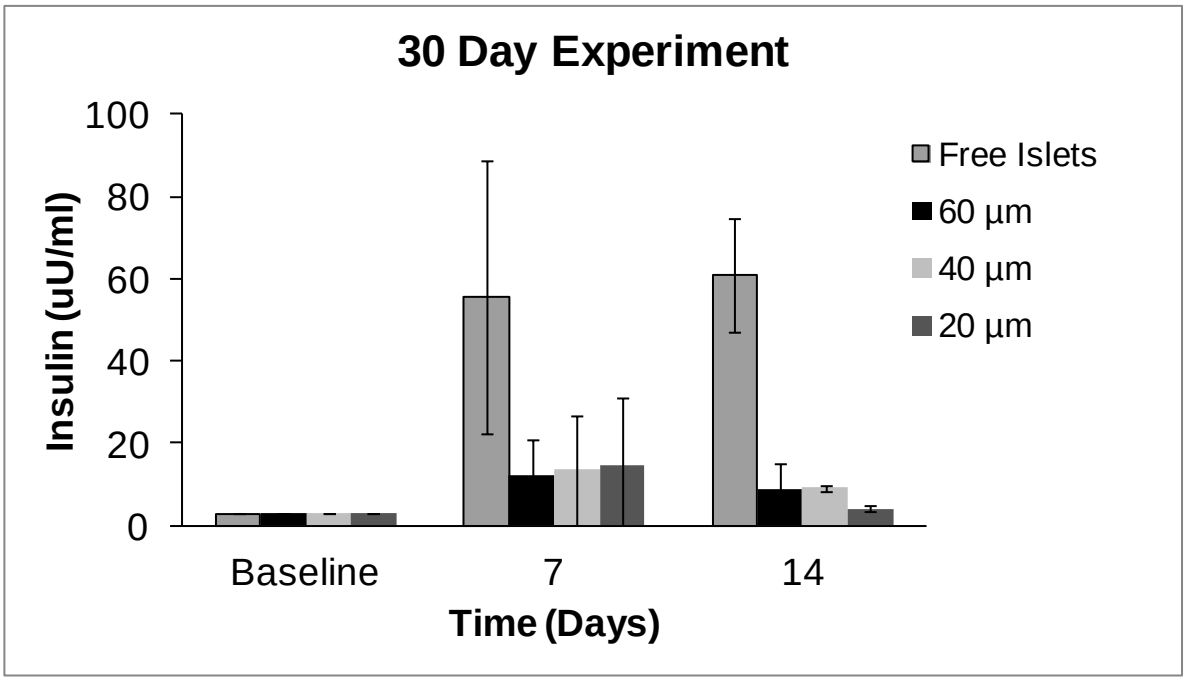

Figure S7. Human insulin levels (presented as mean±SE) were measured 30 minutes post- glucose challenge at day 0 (pre-transplant), day 7 and 14 post-transplant. Levels are reported for all the groups including control group (islets transplanted under the kidney capsule) as well as experimental groups implanted with three different channel size NanoGlands (60, 40 and 20 µm).

Histology

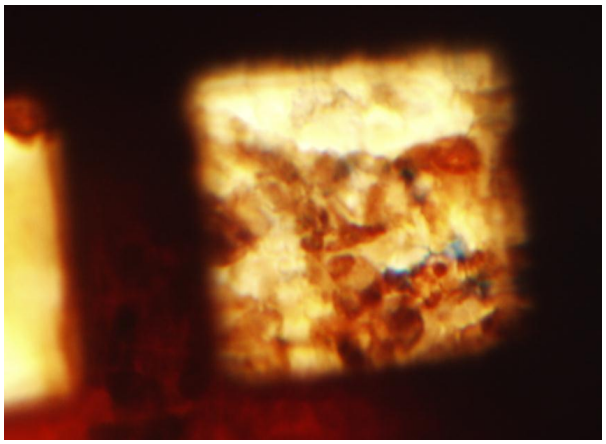

Figure S8. Low- magnification optical microscope image of a 60 µm NanoGland containing human pancreatic islets, retrieved from subcutaneous implantation in nude mice after 4 month. Mice endothelial cells (blue) are infiltrated in pancreatic islet.

Confocal Analysis

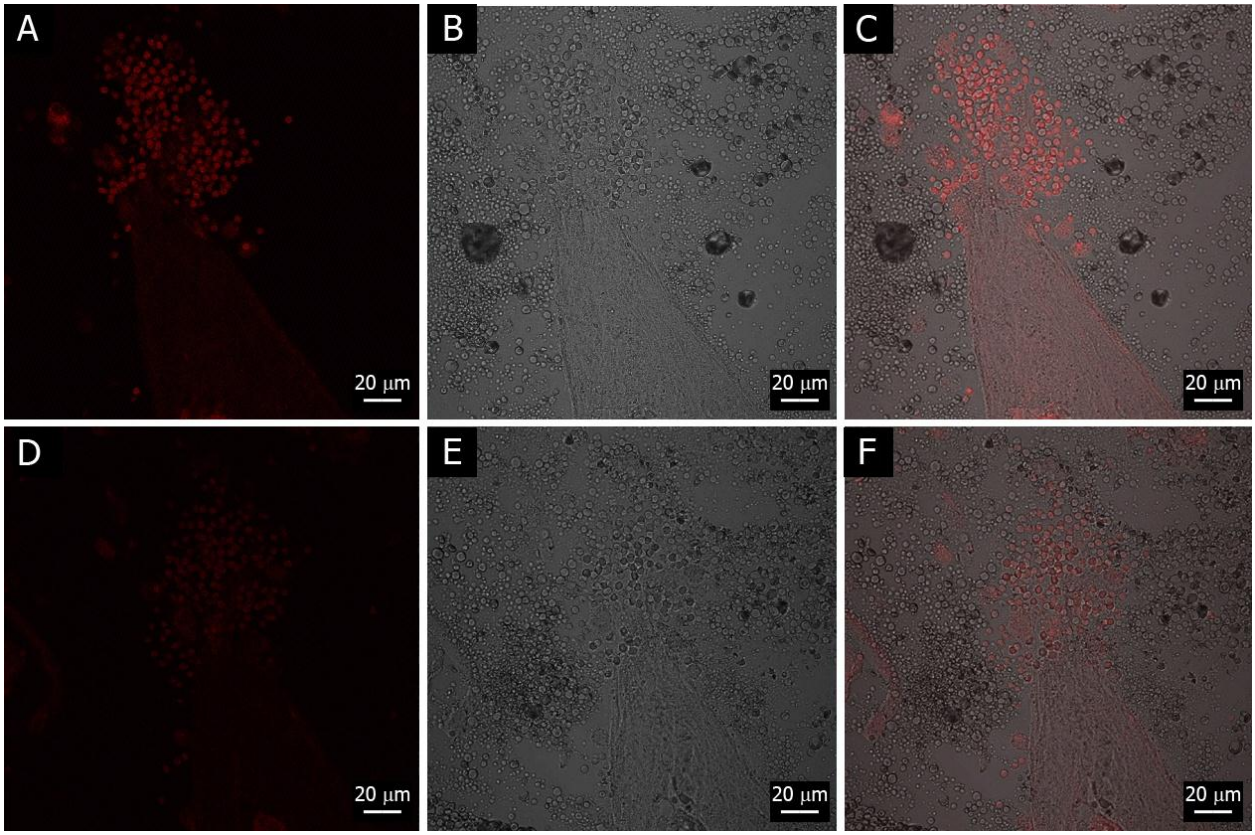

Figure S9. Confocal images of insulin-stained human islets retrieved from a 60 nM template, subcutaneously transplanted in mice for 120 days. 2 sections were taken from the same sample: one was stained with both primary and secondary antibody and the other one was treated with the secondary antibody only as control. Red fluorescent insulin staining (A, D), bright field (B, E) and, overlapped channels (C, F) of stained and control sample, respectively. The positive insulin staining confirms long-term islet viability after transplantation.

References

1. J. K. Gladden and M. Dole, *Journal of the American Chemical Society*, 1953, **75**, 3900-3904. 10.1021/ja01112a008.
2. W. M. Deen, *AIChE Journal*, 1987, **33**, 1409-1425. 10.1002/aic.690330902.
3. J. R. Pappenheimer, E. M. Renkin and L. M. Borrero, *The American journal of physiology*, 1951, **167**, 13-46. http://www.ncbi.nlm.nih.gov/pubmed/14885465.

4. A. Bouchoux, H. R.-d. Balmann and F. Lutin, *Journal of Membrane Science*, 2005, **258**, 123-132. http://dx.doi.org/10.1016/j.memsci.2005.03.002.
5. Stuart and Briegleb, ed. E. L. s. Nachfolger, Germany (Cologne).
6. S. G. Schultz and A. K. Solomon, *The Journal of general physiology*, 1961, **44**, 1189-1199. http://www.ncbi.nlm.nih.gov/pubmed/13748878.
7. A. Ziemys, A. Grattoni, D. Fine, F. Hussain and M. Ferrari, *The Journal of Physical Chemistry B*, 2010, **114**, 11117-11126. 10.1021/jp103519d.
8. A. Ziemys, M. Kojic, M. Milosevic, N. Kojic, F. Hussain, M. Ferrari and A. Grattoni, *J. Comput. Phys.*, 2011, **230**, 5722-5731. 10.1016/j.jcp.2011.03.054.
9. D. E. Harrison, M. R. Christie and D. W. Gray, *Diabetologia*, 1985, **28**, 99-103. http://www.ncbi.nlm.nih.gov/pubmed/3884420.
10. M. Dathe, K. Gast, D. Zirwer, H. Welfle and B. Mehlis, *International journal of peptide and protein research*, 1990, **36**, 344-349. http://www.ncbi.nlm.nih.gov/pubmed/2079389.
11. O. Hosoya, S. Chono, Y. Saso, K. Juni, K. Morimoto and T. Seki, *The Journal of pharmacy and pharmacology*, 2004, **56**, 1501-1507. 10.1211/0022357044878.
12. J. Sih, S. S. Bansal, S. Filipini, S. Ferrati, K. Raghuwansi, E. Zabre, E. Nicolov, D. Fine, M. Ferrari, G. Palapattu and A. Grattoni, *Anal Bioanal Chem*, 2013, **405**, 1547-1557. DOI 10.1007/s00216-012-6484-7.
13. O. M. Sabek, P. Cowan, D. W. Fraga and A. O. Gaber, *Progress in transplantation*, 2006, **16**, 350-354. http://www.ncbi.nlm.nih.gov/pubmed/17183943.
14. O. M. Sabek, D. W. Fraga, O. Minoru, J. L. McClaren and A. O. Gaber, *Transplantation proceedings*, 2005, **37**, 3415-3416. 10.1016/j.transproceed.2005.09.049.
15. A. O. Gaber, D. Fraga, M. Kotb, A. Lo, O. Sabek and K. Latif, *Transplantation proceedings*, 2004, **36**, 1108-1110. 10.1016/j.transproceed.2004.04.055.
16. B. T. Rush, D. W. Fraga, M. Y. Kotb, O. M. Sabek, A. Lo, L. W. Gaber, A. B. Halim and A. O. Gaber, *Transplantation*, 2004, **77**, 1147-1154. http://www.ncbi.nlm.nih.gov/pubmed/15114076.
17. D. W. Fraga, A. O. Gaber and M. Kotb, *Methods in molecular medicine*, 2005, **107**, 303-311. http://www.ncbi.nlm.nih.gov/pubmed/15492381.
18. D. W. Fraga, O. Sabek, D. K. Hathaway and A. O. Gaber, *Transplantation*, 1998, **65**, 1060-1066. http://www.ncbi.nlm.nih.gov/pubmed/9583866.
19. D. W. Fraga, I. Ragueh, S. E. Gebely, O. Sabek, D. K. Hathaway and A. O. Gaber, *Transplantation proceedings*, 1995, **27**, 3279. http://www.ncbi.nlm.nih.gov/pubmed/8539954.

20. A. Osama Gaber, A. Chamsuddin, D. Fraga, J. Fisher and A. Lo, *Transplantation*, 2004, **77**, 309-311. 10.1097/01.TP.0000101509.35249.A0.